Electronic Supplementary Material (ESI) for ChemComm.

Electronic Supporting Information

Table of Contents

1. Materials and methods

All manipulations were carried out under an inert atmosphere of dry nitrogen using standard glovebox and Schlenk techniques. All solvents were taken from the solvent purification machine MB SPS-800 of the company MBRAUN. The ligand complex $[Cp_2Mo_2(CO)_4(\mu,\eta^2\text{-AsSb})]$[1] as well as the metal salts $Cu[FAl\{OC_6F_{10}(C_6F_5)\}_3]\bullet 4CH_3CN$ ($Cu[FAL] \bullet 3.5CH_3CN$)[2] and $Ag[FAl\{OC_6F_{10}(C_6F_5)\}_3]$ (Ag[FAL])[3] were prepared according to literature procedures. Solid state IR spectra were recorded using a ThermoFisher Nicolet iS5 FT-IR spectrometer with an iD7 ATR module and an ITX Diamond crystal. ^1H spectra were recorded on a Bruker Avance 400 spectrometer. ^1H chemical shifts were reported in parts per million (ppm) relative to Me_4Si as external standard. The ESI-MS (ESI = Electrospray ionization) spectra were recorded on a Finnigan Thermoquest TSQ 7000 mass spectrometer with dichloromethane or acetonitrile as solvent. Elemental analyses were performed on an Elementar Vario EL III apparatus by the microanalytical laboratory of the University of Regensburg.

2. Experimental details and characterization

2.1. Synthesis of $[\{\{CpMo(CO)_2\}_2\{\mu, \eta^2:\eta^2\text{-AsSb}\}\}]_2[Cu(\mu\text{-Cl})]_2$ (1):

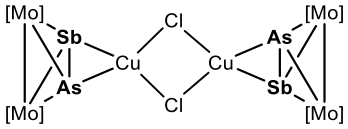

[Mo] = $CpMo(CO)_2$

A solution of CuCl (10 mg, 0.1 mmol) in 5 mL of CH_3CN was slowly layered over a solution of $[Cp_2Mo_2(CO)_4(\mu,\eta^2\text{-SbAs})]$ (**C**) (63 mg, 0.1 mmol) in 5 mL of CH_2Cl_2 at room temperature. Within one week, red crystals of were formed. The product was filtered, washed with CH_2Cl_2 (5 mL) and then dried *in vacuo*. Yield: 49 mg, (68%). ^1H NMR (400 MHz, CD_3CN, 25 °C): δ [ppm] = 5.26 (s, H_{Cp}). ESI-MS (CH_3CN) positive mode: m/z = 1424.2 (0.66%, $[\{Cp_2(CO)_4Mo_2AsSb\}_2Cu_2Cl]^+$), 1324.3 (1.72%, $[\{Cp_2(CO)_4Mo_2AsSb\}_2Cu]^+$), 735.6 (1.03%, $[\{Cp_2(CO)_4Mo_2AsSb\}\{CH_3CN\}Cu]^+$), 144.9 (100%, $\{CH_3CN\}_2Cu$), 103.9 (34%, $\{CH_3CN\}Cu$). Elemental analysis (%) calculated for ($C_{56}H_{40}As_4Cl_4Cu_4Mo_8O_{16}Sb_4$) (2926.37 g·mol^{-1}): C, 22.96; H, 1.38; found: C, 22.53; H, 1.34. IR (Di-ATR): $\tilde{\nu}$ = 1971 (s), 1951 (s), 1900 (s), 1423 (vw), 1351 (m), 1299 (w), 1272 (m), 1239 (vw), 1207 (s), 1159 (w), 1063 (vw), 969 (vs), 822 (s), 724 (vs), 560 (s), 524 (s), 490 (m), 444 (vs).

2.2. Synthesis of $[\{\{CpMo(CO)_2\}_2\{\mu, \eta^2:\eta^2\text{-AsSb}\}\}]_2[Cu(\mu\text{-Br})]_2$ (2):

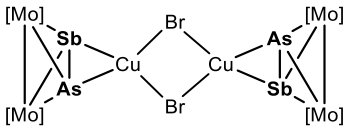

[Mo] = $CpMo(CO)_2$

A solution of CuBr (14 mg, 0.1 mmol) in 5 mL of CH_3CN was slowly layered over a solution of $[Cp_2Mo_2(CO)_4(\mu,\eta^2\text{-SbAs})]$ (**C**) (63 mg, 0.1 mmol) in 5 mL of CH_2Cl_2 at room temperature. Within one week, red crystals of were formed. The product was filtered, washed with CH_2Cl_2 (5 mL) and then dried *in vacuo*. Yield: 54 mg, (70%). ^1H NMR (400 MHz, CD_3CN, 25 °C): δ [ppm] = 5.27 (s, H_{Cp}). ESI-MS (CH_3CN) positive mode: m/z = 1468.2 (0.47%, $[\{Cp_2(CO)_4Mo_2AsSb\}_2Cu_2Br]^+$), 1324.3 (1.22%, $[\{Cp_2(CO)_4Mo_2AsSb\}_2Cu]^+$), 735.6 (0.82%, $[\{Cp_2(CO)_4Mo_2AsSb\}\{CH_3CN\}Cu]^+$), 144.9 (100%, $\{CH_3CN\}_2Cu$), 103.9 (33%, $\{CH_3CN\}Cu$). Elemental analysis (%) calculated for ($C_{56}H_{40}As_4Br_4Cu_4Mo_8O_{16}Sb_4$) (3102.17 g·mol^{-1}): C, 21.66; H, 1.30; found: C, 21.67; H, 1.28. IR (Di-ATR): $\tilde{\nu}$ = 1979 (s), 1946 (s), 1351 (w), 1297 (m), 1275 (vs), 1240 (m), 1215 (vs), 1169 (w), 972 (vs), 828 (s), 726 (vs), 560 (s), 522 (s), 491 (m).

2.3. Synthesis of [{{CpMo(CO)$_2$}$_2${μ, η^2:η^2-AsSb}}]$_2$[Cu(μ-I)]$_2$ (3):

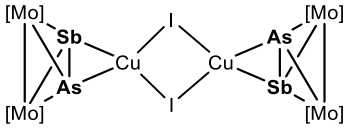

[Mo] = CpMo(CO)$_2$

A solution of CuI (19 mg, 0.1 mmol) in 5 mL of CH_3CN was slowly layered over a solution of [$Cp_2Mo_2(CO)_4$(μ,η^2-SbAs)] (**C**) (63 mg, 0.1 mmol) in 5 mL of CH_2Cl_2 at room temperature. Within one week, red crystals of were formed. The product was filtered, washed with CH_2Cl_2 (5 mL) and then dried *in vacuo*. Yield: 67 mg, (74%). ^{1}H NMR (400 MHz, CD_3CN, 25 °C): δ [ppm] = 5.27 (s, H_{Cp}). ESI-MS (CH_2Cl_2) positive mode: m/z = 1516.2 (0.29%, [{$Cp_2(CO)_4Mo_2AsSb$}$_2Cu_2I$]$^+$), 1324.3 (1.72%, [{$Cp_2(CO)_4Mo_2AsSb$}$_2Cu$]$^+$), 735.6 (1.11%, [{$Cp_2(CO)_4Mo_2AsSb$}{CH_3CN}Cu]$^+$), 144.9 (100%, {CH_3CN}$_2$Cu), 103.9 (34.4%, {CH_3CN}Cu). Elemental analysis (%) calculated for ($C_{14}H_{10}AsCuIMo_2O_4Sb$) (823.53 g·mol^{-1}): C, 20.40; H, 1.22; found: C, 20.64; H, 0.99. IR (Di-ATR): $\tilde{\nu}$ = 1974 (s), 1942 (s), 1876 (vs), 1422 (vw), 1351 (w), 1299 (w), 1276 (s), 1217 (vs), 1161 (vw), 973 (vs), 828 (m), 728 (s).

2.4. [{{CpMo(CO)$_2$}$_2${μ, η^2:η^1:η^2-AsSb}}$_2${CH_3CN}$_3Cu_2$][FAl{$OC_6F_{10}(C_6F_5)$}$_3$]$_2$ (4):

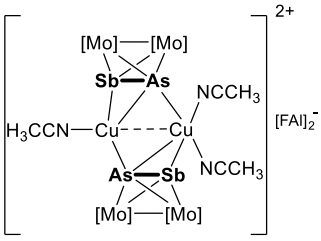

[Mo] = CpMo(CO)$_2$
[FAl] = [FAl{$OC_6F_{10}(C_6F_5)$}$_3$]

A solution of Cu[FAl{$OC_6F_{10}(C_6F_5)$}$_3$] • 3.5CH_3CN (81 mg, 0.05 mmol) in 5 mL of CH_2Cl_2 was slowly added to a stirred solution of [$Cp_2Mo_2(CO)_4$(μ,η^2-SbAs)] (**C**) (31 mg, 0.05 mmol) in 5 mL of CH_2Cl_2 at room temperature. The red solution was stirred for 1 h at room temperature, after which, it was carefully layered with 20 ml if *n*-pentane. Within few days, red crystals of were obtained, filtered, washed with *n*-pentane (5 ml x 2) and dried *in vacuo*. Yield: 69 mg, (61%). ^{1}H NMR (400 MHz, CD_3CN, 25 °C): δ [ppm] = 5.26 (s, H_{Cp}). ESI-MS (CH_2Cl_2) positive mode: m/z = 1324.3 (1.5%, [{$Cp_2(CO)_4Mo_2AsSb$}$_2$Cu]$^+$), 735.6 (1.3%, [{$Cp_2(CO)_4Mo_2AsSb$}{CH_3CN}Cu]$^+$), 144.9 (100%, {CH_3CN}$_2$Cu), 103.9 (35%, {CH_3CN}Cu). ESI-MS (CH_2Cl_2) negative mode: m/z = 1380.9 (100%, [FAl{$OC_6F_{10}(C_6F_5)$}$_3$]$^-$). Elemental analysis (%) calculated for ($Al_2As_2C_{109}Cl_6Cu_2F_{92}H_{35}Mo_4N_3O_{14}Sb_2$) (4529.97 g·mol^{-1}): C, 28.87; H, 0.78, N, 0.93; found: C, 28.81; H, 0.47, N, 0.56. IR (Di-ATR): $\tilde{\nu}$ = 2001 (s), 1978 (s), 1952 (vs), 1929 (vs), 1651 (w), 1529 (m), 1484 (vs), 1423 (vw), 1308 (w), 1266 (w), 1239 (m), 1201 (m), 1182 (m), 1149 (m), 1127 (m), 1099 (s), 1062 (vw), 1034 (w), 1000(vs), 951 (vs), 909 (s), 848 (m), 830 (m), 813 (m), 664 (w), 632 (m), 622 (m), 598 (m), 557 (w), 514 (s), 468 (w), 451 (s), 437 (s).

2.4. [{{CpMo(CO)$_2$}$_2${μ, η^2:η^2-AsSb}}$_2${CH_3CN}Cu][FAl{$OC_6F_{10}(C_6F_5)$}$_3$] (5):

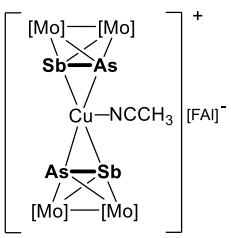

[Mo] = CpMo(CO)$_2$
[FAl] = [FAl{$OC_6F_{10}(C_6F_5)$}$_3$]

A solution of $Cu[FAl\{OC_6F_{10}(C_6F_5)\}_3] \bullet 3.5CH_3CN$ (81 mg, 0.05 mmol) in 5 mL of CH_2Cl_2 was slowly added to a stirred solution of $[Cp_2Mo_2(CO)_4(\mu,\eta^2\text{-SbAs})]$ (**C**) (63 mg, 0.1 mmol) in 8 mL of CH_2Cl_2 at room temperature. The red solution was stirred for 1 h at room temperature, after which, it was carefully layered with 20 ml of *n*-pentane. Within few days, red crystals of were obtained, filtered, washed with *n*-pentane (5 ml x 2) and dried *in vacuo*. Yield: 92 mg, (65%). ^{1}H NMR (400 MHz, CD_3CN, 25 °C): δ [ppm] = 5.27 (s, H_{Cp}). ESI-MS (CH_2Cl_2) positive mode: m/z = 1324.3 (1.9%, $[\{Cp_2(CO)_4Mo_2AsSb\}_2Cu]^+$), 735.6 (1.2%, $[\{Cp_2(CO)_4Mo_2AsSb\}\{CH_3CN\}Cu]^+$), 144.9 (100%, $\{CH_3CN\}_2Cu$), 103.9 (31%, $\{CH_3CN\}Cu$). ESI-MS (CH_2Cl_2) negative mode: m/z = 1380.9 (100%, $[FAl\{OC_6F_{10}(C_6F_5)\}_3]^-$). Elemental analysis (%) calculated for ($C_{67}H_{25}AlAs_2Cl_2CuF_{46}Mo_4NO_{11}Sb_2$) (2836,19 g·mol^{-1}): C, 28.35; H, 0.89; N, 0.49 found: C, 28.93; H, 0.74; N, 0.41. IR (Di-ATR): $\tilde{\nu}$ = 1952 (b, vs), 1933 (b, vs), 1651 (w), 1531 (m), 1481 (vs), 1423 (vw), 1308 (m), 1267 (w), 1242 (w), 1200 (s), 1184 (m), 1151 (w), 1131 (m), 1103 (m), 1065 (vw), 1032 (vw), 1000(s), 953 (vs), 908 (m), 825 (m), 766 (m), 750.4 (m), 727 (m), 668 (vw), 646 (vw), 631 (m), 625 (m), 601 (m), 560 (m), 525 (s), 492 (w), 441 (vs).

2.4. $[\{\{CpMo(CO)_2\}_2\{\mu,\eta^2:\eta^2\text{-AsSb}\}\{\mu,\eta^2:\eta^2:\eta^1\text{-AsSb}\}\}_2Ag_2][FAl\{OC_6F_{10}(C_6F_5)\}_3]_2$ (6):

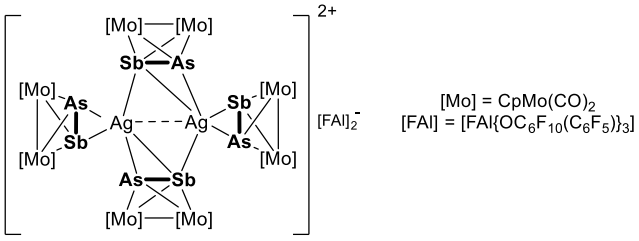

A solution of $Ag[FAl\{OC_6F_{10}(C_6F_5)\}_3]$ (76 mg, 0.05 mmol) in 7 mL of CH_2Cl_2 was slowly added to a stirred solution of $[Cp_2Mo_2(CO)_4(\mu,\eta^2\text{-SbAs})]$ (**C**) (63 mg, 0.1 mmol) in 8 mL of CH_2Cl_2 at room temperature. The red solution was stirred for 1 h at room temperature, after which, it was carefully layered with 20 ml if *n*-pentane. Within few days, red crystals of were obtained, filtered, washed with *n*-pentane (5 ml x 2) and dried *in vacuo*. Yield: 72 mg, (52%). ^{1}H NMR (400 MHz, CD_3CN, 25 °C): δ [ppm] = 5.36 (s, H_{Cp}). ESI-MS (CH_2Cl_2) positive mode: m/z = 1370.3 (100%, $[\{Cp_2(CO)_4Mo_2AsSb\}_2Ag]^+$. ESI-MS ($CH_2Cl_2$) negative mode: m/z = 1380.9 (100%, $[FAl\{OC_6F_{10}(C_6F_5)\}_3]^-$). Elemental analysis (%) calculated for ($C_{129}H_{42}Ag_2Al_2As_4Cl_2F_{92}Mo_8O_{22}Sb_4$) (5594.33 g·mol^{-1}): C, 27.67; H, 0.76; found: C, 28.05; H, 0.77. IR (Di-ATR): $\tilde{\nu}$ = 1954 (b, vs), 1931 (b, vs), 1920 (vs, b), 1651 (w), 1531 (m), 1482 (vs), 1423 (vw), 1322 (m), 1307 (m), 1267 (w), 1242 (w), 1201 (s), 1189 (m), 1153 (w), 1132 (w), 1103 (m), 1065 (vw), 1035 (vw), 1014 (s), 1001(s), 952 (vs), 909 (m), 829 (s), 767 (m), 749 (w), 728 (m), 666 (vw), 624 (m), 599 (w), 560 (m), 523 (s), 490 (w), 440 (vs).

3. Crystallographic details

Suitable crystals were selected and mounted on a Gemini Ultra diffractometer equipped with an AtlasS2 CCD detector (**1**, **2**, **3**, **6**) or on a SuperNova diffractometer equipped with an TitanS2 CCD detector (**4**, **5**). The crystals were kept at a steady T = 123(1) during data collection. Data collection and reduction were performed with CrysAlisPro.[4] For the compounds **1**, **4** and **5** a numerical absorption correction based on a gaussian integration over a multifaceted crystal model and an empirical absorption correction using spherical harmonics, as implemented in SCALE3 ABSPACK scaling algorithm, was applied. For the compounds **2**, **3** and **6** an analytical numeric absorption correction using a multifaceted crystal model based on expressions derived by R.C. Clark & J.S. Reid.[5] and an empirical absorption correction using spherical harmonics, as implemented in SCALE3 ABSPACK scaling algorithm, was applied. Using Olex2,[6] the structures were solved with ShelXT[7] and a least-square refinement on F^2 was carried out with ShelXL[8] for all structures. All non-hydrogen atoms were refined anisotropically. Hydrogen atoms at the carbon atoms were located in idealized positions and refined isotropically according to the riding model.

Figures were created with Olex2.[6]

Compound 1: The asymmetric unit contains two molecules of $[\{\{CpMo(CO)_2\}_2(\mu,\eta^2{:}\eta^2{:}\eta^2\text{-}AsSb)\}]_2[Cu(\mu\text{-}Cl)]_2$ (**1**). The As-Sb units of all four $[\{\{CpMo(CO)_2\}_2(\mu,\eta^2{:}\eta^2{:}\eta^2\text{-}AsSb)\}]$ fragments are disordered over two positions with occupancies of 0.57 to 0.43, 0.53 to 0.47, 0.53 to 0.47 and 0.59 to 0.41, respectively. The SIMU restraint was applied to refine these disorders. Further, the crystal was twinned and was therefore refined as a 2-component twin (BASF: 0.7764(11) and 0.2236(11)).

Compound 2: The asymmetric unit contains two molecules of $[\{\{CpMo(CO)_2\}_2(\mu,\eta^2{:}\eta^2{:}\eta^2\text{-}AsSb)\}]_2[Cu(\mu\text{-}Br)]_2$ (**2**). The As-Sb units of all four $[\{\{CpMo(CO)_2\}_2(\mu,\eta^2{:}\eta^2{:}\eta^2\text{-}AsSb)\}]$ fragments are disordered over two positions with occupancies of 0.61 to 0.39, 0.57 to 0.43, 0.54 to 0.46 and 0.56 to 0.44, respectively. Further are the four Br atoms disordered over two positions with occupancies of 0.82 to 0.18, 0.71 to 0.29, 0.78 to 0.22 and 0.55 to 0.45, respectively. The restraints SADI and SIMU were used to describe these disorders.

Compound 3: The asymmetric unit contains half a molecule of $[\{\{CpMo(CO)_2\}_2(\mu,\eta^2{:}\eta^2{:}\eta^2\text{-}AsSb)\}]_2[Cu(\mu\text{-}I)]_2$ (**3**) (which lies about an inversion center) and one CH_2Cl_2 solvent molecule. The As-Sb unit of the $[\{\{CpMo(CO)_2\}_2(\mu,\eta^2{:}\eta^2{:}\eta^2\text{-}AsSb)\}]$ fragment is disordered over two positions with occupancies of 0.66 to 0.34. Further is the CH_2Cl_2 solvent molecule disordered over two positions (0.62:0.38). The restraints SIMU and SADI were applied to model the disorder of the CH_2Cl_2 solvent molecule.

Compound 4: The asymmetric unit contains the dication $[\{\{CpMo(CO)_2\}_2\{\mu,\eta^2{:}\eta^2{:}\eta^1{:}\eta^2\text{-}AsSb\}\}_2\{CH_3CN\}_3Cu^2]^{2+}$, two $[FAl\{OC_6F_{10}(C_6F_5)\}_3]^-$ anions and 2.8 CH_2Cl_2 solvent molecule. The $[\{\{CpMo(CO)_2\}_2(\mu,\eta^2{:}\eta^2{:}\eta^2\text{-}AsSb)\}]$ fragments show disorder over three positions. However, the ligand Cp and CO ligands could only be modelled over two and one position, respectively. Further, one of the CH_3CN molecules coordinated to Cu1 is disordered (0.56:0.44). 1.8 of the three CH_2Cl_2 solvent molecules were heavily disordered. Therefore, a solvent mask was calculated. The third CH_2Cl_2 solvent molecule is disordered over two positions (0.58:0.42). Adequate restraints were used to describe these disorders.

Compound 5: The asymmetric unit contains the cation $[\{\{CpMo(CO)_2\}_2\{\mu,\eta^2{:}\eta^2{:}\eta^2\text{-}AsSb\}\}_2\{CH_3CN\}Cu]^+$, the anion $[FAl\{OC_6F_{10}(C_6F_5)\}_3]^-$ and a CH_2Cl_2 solvent molecule. The As-Sb units of both $[\{\{CpMo(CO)_2\}_2(\mu,\eta^2{:}\eta^2{:}\eta^2\text{-}AsSb)\}]$ fragments are disordered over two positions with occupancies of 0.66 to 0.34 and 0.70 to 0.30, respectively. Further is the CH_2Cl_2 solvent molecule disordered over two positions (0.73:0.27). The restraints SIMU and SADI were applied to model these disorders.

Compound 6: The asymmetric unit contains the dication $[\{\{CpMo(CO)_2\}_2\{\mu,\eta^2{:}\eta^2{:}\eta^2\text{-}AsSb\}\{\mu,\eta^2{:}\eta^2{:}\eta^2{:}\eta^1\text{-}AsSb\}\}_2Ag_2]^{2+}$, two molecules of the anion $[FAl\{OC_6F_{10}(C_6F_5)\}_3]^-$ and a Ch2Cl2 solvent molecule. The As-Sb units of all four $[\{\{CpMo(CO)_2\}_2(\mu,\eta^2{:}\eta^2{:}\eta^2\text{-}AsSb)\}]$ fragments are disordered over two positions with occupancies of 0.86 to 0.14, 0.80 to 0.20, 0.65 to 0.35 and 0.72 to 0.28, respectively.

Further is the Ag2 atom disordered over two positions (0.62:0.32). Additionally is one of the [$CoMo(CO)_2$] fragments disordered over two positions (0.53:0.47). The restraints SIMU and SADI were applied to model these disorders.

CCDC-2330295 (**1**), CCDC-2330296 (**2**), CCDC-2330297 (**3**), CCDC-2330298 (**4**), CCDC-2330299 (**5**) and CCDC-2330300 (**6**) contain the supplementary crystallographic data for this paper. These data can be obtained free of charge at www.ccdc.cam.ac.uk/conts/retrieving.html (or from the Cambridge Crystallographic Data Centre, 12 Union Road, Cambridge CB2 1EZ, UK; Fax: + 44-1223-336-033; email: deposit@ccdc.cam.ac.uk).

Table S1. Crystallographic data for compounds **1**-**4**.

Compound	**1**	**2**	**3**·2 CH_2Cl_2	**4**·3 CH_2Cl_2
Data set (internal naming)	test2abs_twin1_hklf4	ems_634_2_ap_abs	ems_635_mP_abs	PSH_132_mP_testabs
CCDC number	2330295	2330296	2330297	2330298
Formula	$C_{56}H_{40}As_4Cl_4Cu_4Mo_8O_{16}Sb_4$	$C_{56}H_{40}As_4Br_4Cu_4Mo_8O_{16}Sb_4$	$C_{15}H_{12}AsCl_2CuIMo_2O_4Sb$	$Al_2As_2C_{109}Cl_6Cu_2F_{92}H_{35}Mo_4N_3O_{14}Sb_2$
$D_{calc.}$ / g · cm^{-3}	2.648	2.785	2.740	2.153
μ/mm^{-1}	5.898	7.867	6.448	9.595
Formula Weight	2919.04	3096.88	906.14	4529.24
Colour	red	red	red	orange
Shape	block	block	plate	plate
Size/mm^3	0.13×0.11×0.09	0.21×0.20×0.10	0.18×0.16×0.04	0.67×0.31×0.07
T/K	123(1)	123(1)	123(1)	123.01(10)
Crystal System	triclinic	triclinic	monoclinic	monoclinic
Space Group	*P*-1	*P*-1	$P2_1/n$	$P2_1/n$
a/Å	15.0550(6)	14.9733(4)	10.4347(4)	23.6343(3)
b/Å	15.1827(9)	15.0851(5)	15.6404(6)	19.0078(2)
c/Å	17.1422(4)	17.3390(5)	13.4725(4)	31.4538(3)
α/°	89.358(3)	89.022(2)	90	90
β/°	89.116(3)	88.933(2)	92.374(3)	98.5123(11)
γ/°	69.160(4)	70.588(3)	90	90
V/$Å^3$	3661.4(3)	3692.9(2)	2196.86(14)	13974.5(3)
Z	2	2	4	4
Z'	1	1	1	1
Wavelength/Å	0.71073	0.71073	0.71073	1.54184
Radiation type	MoK_α	MoK_α	MoK_α	Cu K_α
θ_{min}/°	3.114	3.319	3.256	3.435
θ_{max}/°	32.486	32.478	32.472	74.554
Measured Refl.	26111	47078	13681	77578
Independent Refl.	26111	23201	7011	27430
Reflections with I > 2(I)	25134	19680	5969	25179
R_{int}	0.0499	0.0301	0.0332	0.0532
Parameters	942	1000	291	2303
Restraints	144	16	60	457
Largest Peak	2.730	1.133	1.672	2.539
Deepest Hole	-1.717	-1.127	-1.353	-2.480
GooF	1.262	1.247	1.075	1.064
wR_2 (all data)	0.1753	0.0801	0.0840	0.2085
wR_2	0.1727	0.0769	0.0796	0.2050
R_1 (all data)	0.0754	0.0561	0.0479	0.0827
R_1	0.0717	0.0430	0.0374	0.0787

Table S2. Crystallographic data for compounds **5**-**6**.

Compound	**5**· CH_2Cl_2	**6**· CH_2Cl_2
Data set (internal naming)	PSH_133_mP_abs_gaus	PSH_141_mP_abs_ana
CCDC number	2330299	2330300
Formula	$C_{67}H_{25}AlAs_2Cl_2CuF_{46}Mo_4NO_{11}Sb_2$	$C_{129}H_{42}Ag_2Al_2As_4Cl_2F_{92}Mo_8O_{22}Sb_4$
$D_{calc.}$ / g · cm^{-3}	2.303	2.378
μ/mm^{-1}	13.448	15.419
Formula Weight	2832.40	5586.42
Colour	clear dark orange	clear dark red
Shape	block	block
Size/mm^3	0.75×0.40×0.09	0.27×0.22×0.18
T/K	123.00(10)	123(1)
Crystal System	monoclinic	monoclinic
Space Group	$P2_1/c$	$P2_1/n$
a/Å	20.9582(2)	11.46640(10)
b/Å	33.3030(4)	40.5323(3)
c/Å	12.1289(2)	33.5837(2)
α/°	90	90
β/°	105.2370(10)	91.7040(10)
γ/°	90	90
V/Å^3	8168.03(19)	15601.4(2)
Z	4	4
Z'	1	1
Wavelength/Å	1.54184	1.54184
Radiation type	Cu K_a	Cu K_a
θ_{min}/°	3.438	3.419
θ_{max}/°	74.061	71.725
Measured Refl.	36804	66428
Independent Refl.	15774	29653
Reflections with I > 2(I)	14735	27646
R_{int}	0.0433	0.0333
Parameters	1302	2548
Restraints	97	164
Largest Peak	1.265	1.699
Deepest Hole	-1.284	-1.811
GooF	1.063	1.072
wR_2 (all data)	0.1255	0.1137
wR_2	0.1231	0.1114
R_1 (all data)	0.0497	0.0441
R_1	0.0467	0.0414

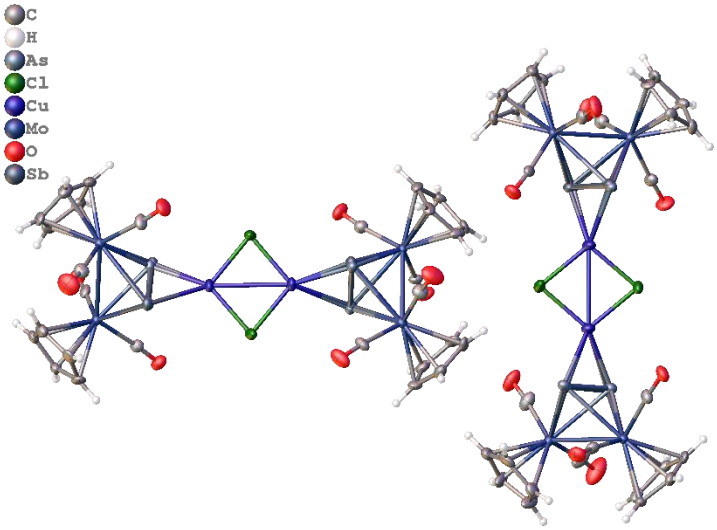

Fig. S1. View of the asymmetric unit of **1**.

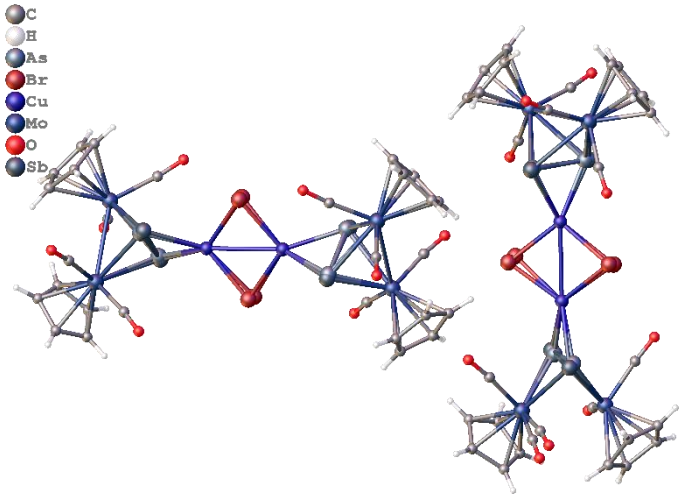

Fig. S2. View of the asymmetric unit of **2**.

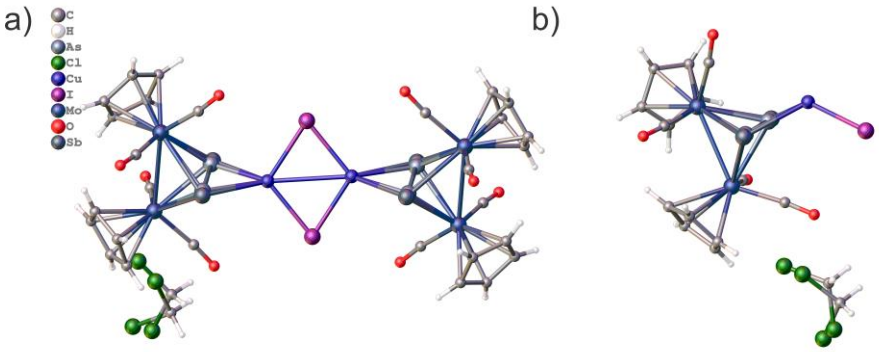

Fig. S3. a) Molecular structure of compound **3** in the solid state; b) View of the asymmetric unit of **3**.

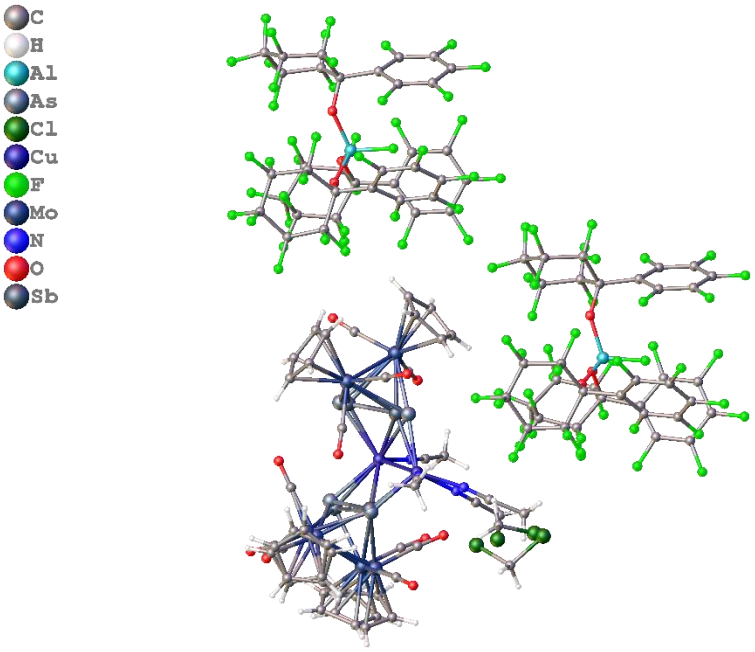

Fig. S4. View of the asymmetric unit of **4**.

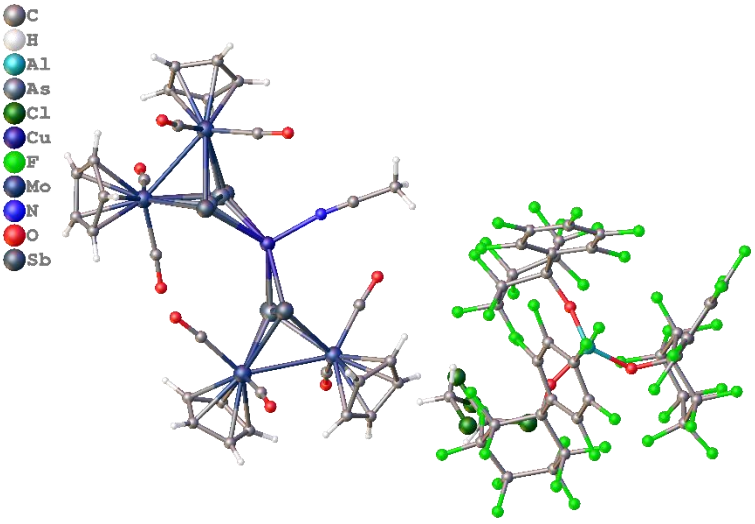

Fig. S5. View of the asymmetric unit of **5**.

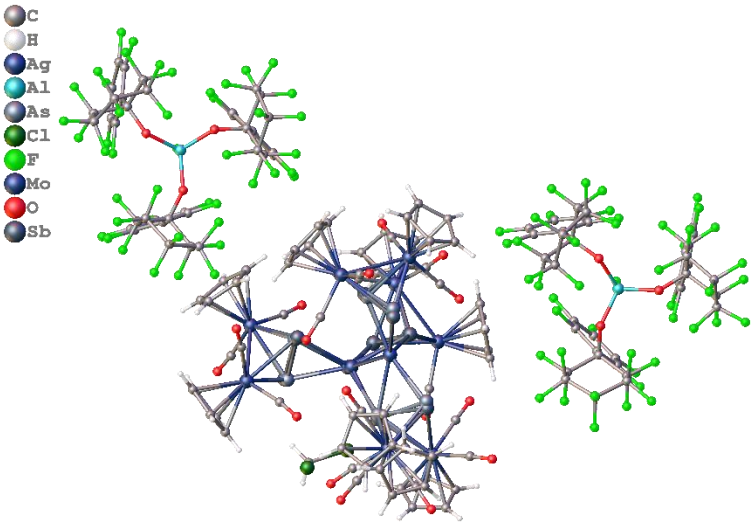

Figure S6. View of the asymmetric unit of **6**.

4. Computational details

4.1. General information

The DFT calculations have been performed with Gaussian 09 program package.[9] For the cationic part of **6**, the BP86[10]/def2-SVP[11] level of theory with Grimme's dispersion correction with BJ-damping (GD3BJ)[12] was used. As the cationic part of **6** shows some disorder in its X-ray structure, two linkage isomers $[(\mu_{Sb},\eta^{2:1}\text{-}\mathbf{C})_2(\eta^2\text{-}\mathbf{C})_2Ag_2]^{2+}$ (parts 0 and 1 in the X-ray structure) and $[(\mu_{As},\eta^{2:1}\text{-}\mathbf{C})_2(\eta^2\text{-}\mathbf{C})_2Ag_2]^{2+}$ (parts 0 and 2 in the X-ray structure) (subscript after "μ" indicates bridging atom of the $\eta^{2:1}$-**C** complex in these linkage isomers) were optimized and analyzed separately (see details below). DDEC6 bond orders[13] were calculated using the Chargemol software, QTAIM[14] and IRI[15] analysis were performed using the Multiwfn software.[16]

For the NBO analysis of $[(C_5H_5)_2Mo_2(CO_4)(\mu,\eta^2\text{-AsSb})]$ (**C**), the geometry was optimized on the B3LYP[17]/def2-TZVP[11] level of theory (see details below). Natural Bonding Orbitals (NBOs) were generated using NBO7 program package.[18]

The minimum nature of the optimized geometry of all compounds has been proven by calculating the vibration spectrum, which shows no imaginary frequencies. All optimized geometries are listed in the corresponding section of the supporting information. They can also be found in a supplemented multi-xyz file.

4.2. Natural Bonding Orbital (NBO) Analysis

Natural Bonding Orbitals (NBOs) of $[(C_5H_5)_2Mo_2(CO)_4(\mu,\eta^2\text{-AsSb})]$ (**C**) for orbital energy diagram were generated using NBO7 program package on the B3LYP/def2-TZVP level of theory. The NBO data of $[(C_5H_5)_2Mo_2(CO)_4(\mu,\eta^2\text{-As}_2)]$ (**A**) and $[(C_5H_5)_2Mo_2(CO)_4(\mu,\eta^2\text{-Sb}_2)]$ (**B**) calculated on the same level of theory were adapted from our previous publications.[19] Selected NBOs of compound **C** are summarized in Table S3.

Table S3. Selected Natural Bond Orbitals (NBOs) for compound $[(C_5H_5)_2Mo_2(CO)_4(\mu,\eta^2\text{-AsSb})]$ (**C**) calculated at the B3LYP/def2-TZVP level of theory. BD stands for sigma bonds; LP stands for lone pairs. The asterisk indicates antibonding orbitals.

Orbital	Energy, eV
LP (1)Sb 32	-11.349
LP (1)As 16	-11.633
BD (1)As 16-Sb 32	-7.917
BD (1)Mo 1-As 16	-7.211
BD (1)Mo 1-Sb 32	-6.452
BD (1)As 16-Mo 17	-7.131
BD (1)Mo 17-Sb 32	-6.459
BD (1)Mo 1-Mo 17	-4.705
BD*(1)Mo 1-Mo 17	-0.764
BD*(1)Mo 1-As 16	2.173
BD*(1)Mo 17-Sb 32	1.512
BD*(1)As 16-Mo 17	0.835
BD*(1)Mo 1-Sb 32	0.498
BD*(1)As 16-Sb 32	1.089

4.3. Density Derived Electrostatic and Chemical (DDEC) Bond Order Calculations

Bond orders (BOs) for compounds $[(\mu_{Sb},\eta^{2:1}\text{-}\mathbf{C})_2(\eta^2\text{-}\mathbf{C})_2Ag_2]^{2+}$ and $[(\mu_{As},\eta^{2:1}\text{-}\mathbf{C})_2(\eta^2\text{-}\mathbf{C})_2Ag_2]^{2+}$ were calculated using Density Derived Electrostatic and Chemical (DDEC6) approach using the Chargemol program package on the BP86/def2-SVP level of theory with Grimme's dispersion correction with BJ-damping (GD3BJ) (Figure S7, Tables S4). For both structures, notable non-zero (0.1537-0.1700) BOs between Ag^{I} ions were observed suggesting the presence of argentophilic interactions.

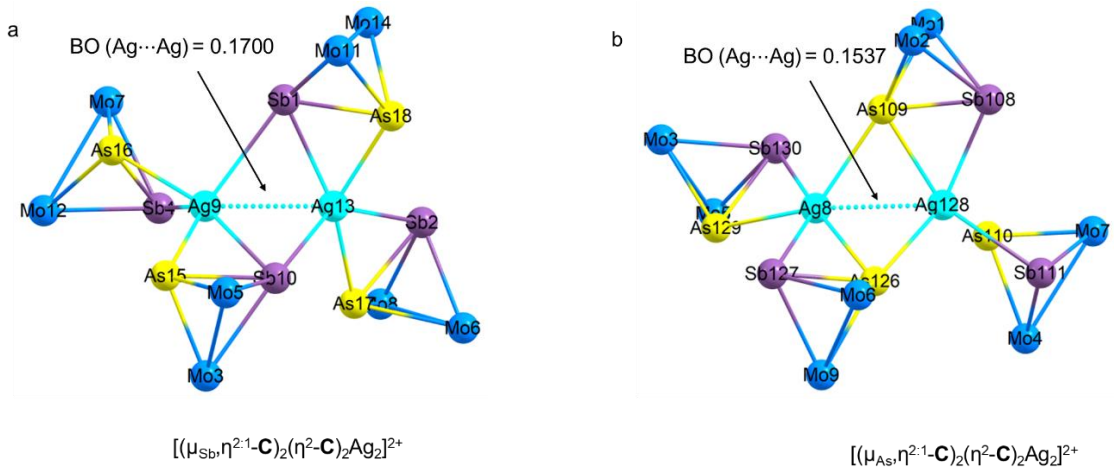

$[(\mu_{Sb},\eta^{2:1}\text{-}\mathbf{C})_2(\eta^2\text{-}\mathbf{C})_2Ag_2]^{2+}$ $[(\mu_{As},\eta^{2:1}\text{-}\mathbf{C})_2(\eta^2\text{-}\mathbf{C})_2Ag_2]^{2+}$

Figure S7 Optimized structures of $[(\mu_{Sb},\eta^{2:1}\text{-}\mathbf{C})_2(\eta^2\text{-}\mathbf{C})_2Ag_2]^{2+}$ (a) and $[(\mu_{As},\eta^{2:1}\text{-}\mathbf{C})_2(\eta^2\text{-}\mathbf{C})_2Ag_2]^{2+}$ (b) with corresponding BO indexes corresponding to Ag···Ag interactions. C, H, and O atoms are omitted for clarity.

Table S4 Summary of the Bond Order (BO) analysis of spicies $[(\mu_{Sb},\eta^{2:1}\text{-}\mathbf{C})_2(\eta^2\text{-}\mathbf{C})_2Ag_2]^{2+}$ and $[(\mu_{As},\eta^{2:1}\text{-}\mathbf{C})_2(\eta^2\text{-}\mathbf{C})_2Ag_2]^{2+}$ calculated at the BP86/def2-SVP (GD3BJ) level of theory usin DDCE6 approach.

Species	As-Sb BOs		Ag···Ag BOs	
$[(\mu_{Sb},\eta^{2:1}\text{-}\mathbf{C})_2(\eta^2\text{-}\mathbf{C})_2Ag_2]^{2+}$	As15-Sb10	0.6572	Ag9-Ag13	0.1700
	As16-Sb4	0.6873		
	As17-Sb2	0.6590		
	As18-Sb1	0.6803		
$[(\mu_{As},\eta^{2:1}\text{-}\mathbf{C})_2(\eta^2\text{-}\mathbf{C})_2Ag_2]^{2+}$	As109-Sb-108	0.6901	Ag8-Ag128	0.1537
	As110-Sb111	0.7076		
	As126-Sb127	0.6926		
	As129-Sb130	0.6733		

4.4. Interaction Region Indicators (IRI) Analysis

The Interaction Region Indicator (IRI) analysis was performed using the Multiwfn program package (version 3.8) on the BP86/def2-SVP level of theory (with GD3BJ) for compounds $[(\mu_{Sb},\eta^{2:1}\text{-}\mathbf{C})_2(\eta^2\text{-}\mathbf{C})_2Ag_2]^{2+}$ and $[(\mu_{As},\eta^{2:1}\text{-}\mathbf{C})_2(\eta^2\text{-}\mathbf{C})_2Ag_2]^{2+}$. IRI isosurfaces (isovalue = 1.0) were mapped with sign(λ_2)ρ function (Figure S8a and S9a). Visual analysis indicates slightly negative sign(λ_2)ρ values in the space between Ag^I ions were attributable to argentophilic interactions. The Isosurfaces were plotted using Chemcraft program package.[20]

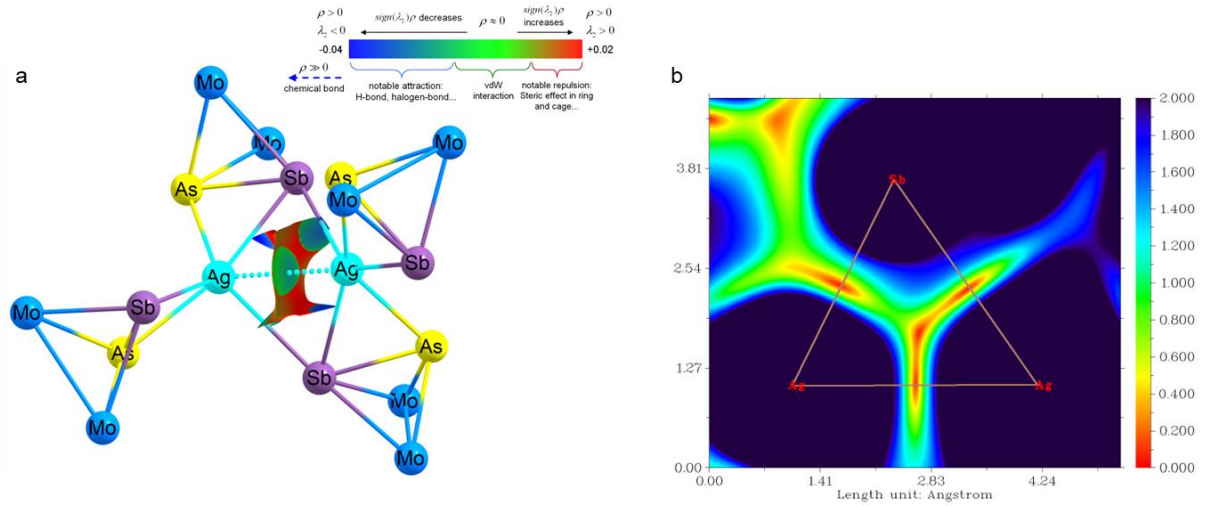

Figure S8 Summary of the IRI analysis for $[(\mu_{Sb},\eta^{2:1}\text{-}\mathbf{C})_2(\eta^2\text{-}\mathbf{C})_2Ag_2]^{2+}$. IRI isosurfaces (isovalue = 1.0) mapped with sign(λ2)ρ values. Negative (bluish) areas correspond to attractive interactions. C, H, and O atoms are not depicted (a); Projection of IRI on plane containing Ag(I) ions (areas with IRI<1 show regions where interactions (these can be both attractive and repulsive) are present).

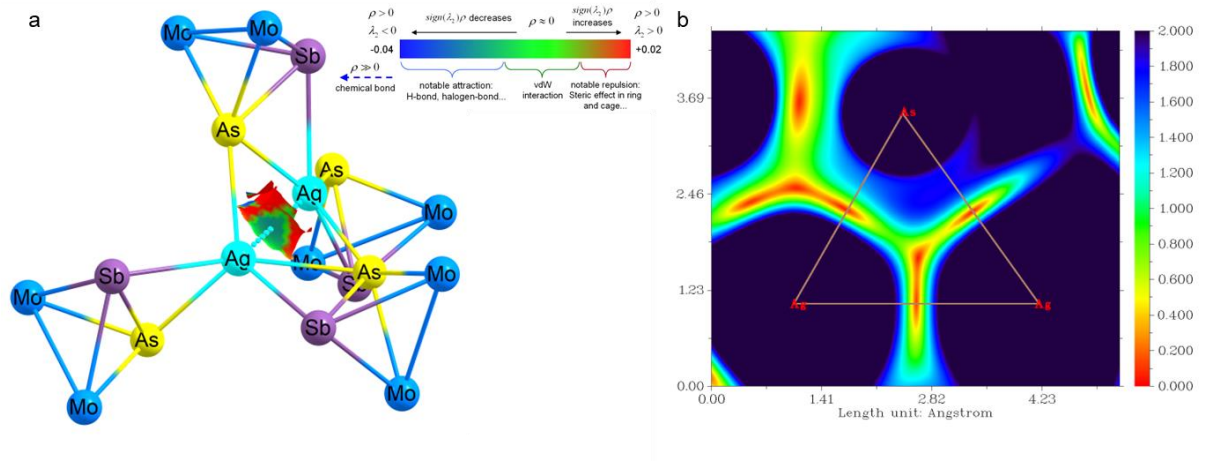

Figure S9 Summary of the IRI analysis for $[(\mu_{As},\eta^{2:1}\text{-}\mathbf{C})_2(\eta^2\text{-}\mathbf{C})_2Ag_2]^{2+}$. IRI isosurfaces (isovalue = 1.0) mapped with sign(λ2)ρ values. Negative (bluish) areas correspond to attractive interactions. C, H, and O atoms are not depicted (a); Projection of IRI on plane containing Ag(I) ions (areas with IRI<1 show regions where interactions (these can be both attractive and repulsive) are present).

4.5. Quantum Theory of Atom in Molecules (QTAIM) analysis

The Quantum Theory of Atom in Molecules (QTAIM) analysis was performed as implemented in Multiwfn program package (version 3.8) on the BP86/def2-SVP level of theory (with GD3BJ) for compounds $[(\mu_{Sb},\eta^{2:1}\text{-}\mathbf{C})_2(\eta^2\text{-}\mathbf{C})_2Ag_2]^{2+}$ and $[(\mu_{As},\eta^{2:1}\text{-}\mathbf{C})_2(\eta^2\text{-}\mathbf{C})_2Ag_2]^{2+}$. In both cases, the analysis shows (3,-1) critical points between neighboring Ag(I) ions serving as an additional indication of the presence of argentophilic interactions (Figures S10-S11). Figures were prepared using Multiwfn and Chemcraft program packages. It is worth mentioning that even though the QTAIM analysis is commonly used as a method for detection of chemical bonds some recent studies suggest that equating the presence of (3,−1) critical points and the existence of a chemical bond between respective atoms can lead to inconsistencies.[21]

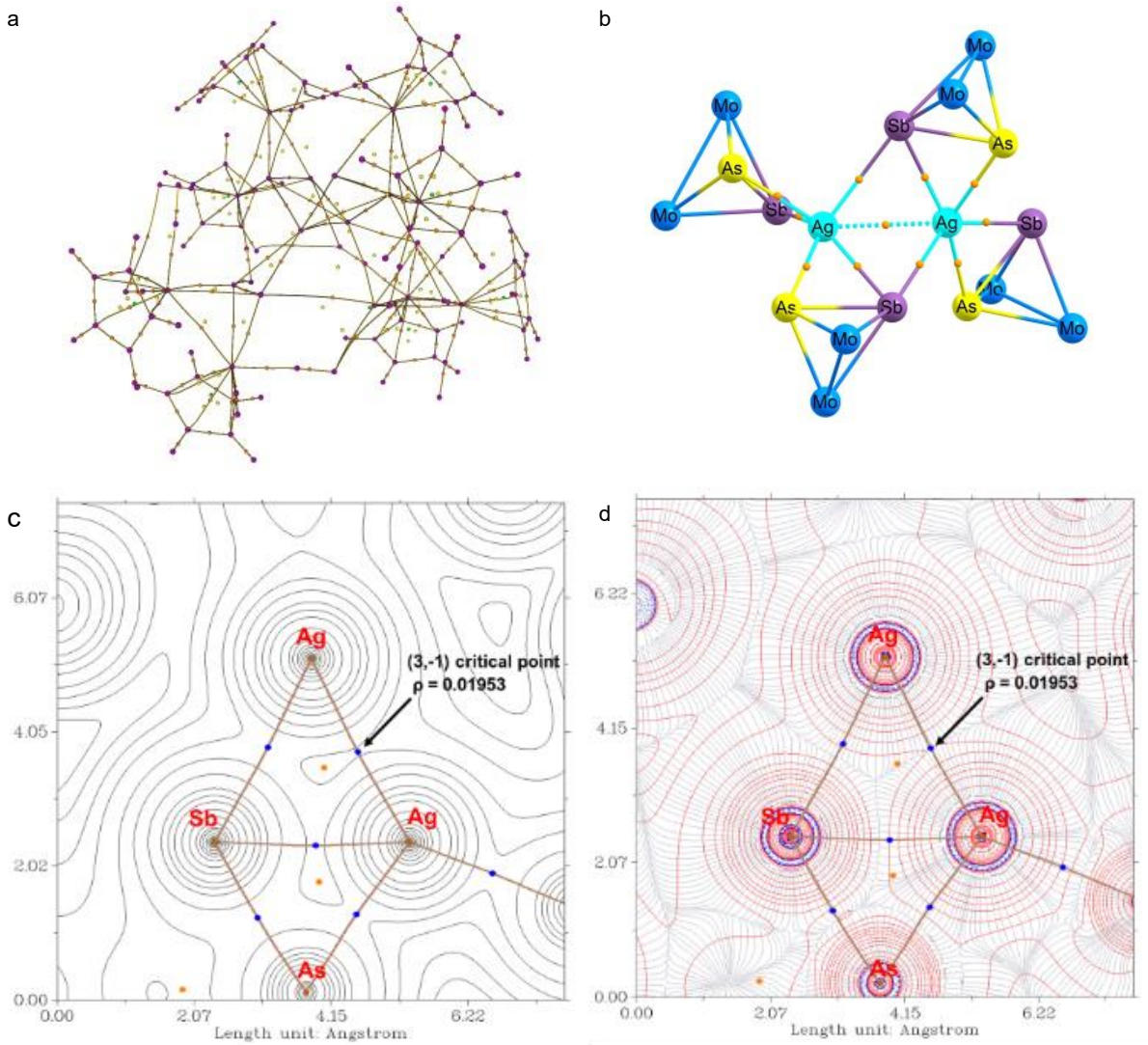

Figure S10 Summary of the QTAIM analysis of the complex $[(\mu_{Sb},\eta^{2:1}\text{-}\mathbf{C})_2(\eta^2\text{-}\mathbf{C})_2Ag_2]^{2+}$. Molecular graph, showing the bond (3,-3) (purple), (3,-1) (orange), (3,+1) (yellow) and (3,+3) (green) critical points (a). Heavy atom core of the complex overlayed with selected (3,-1) bond critical points closest to the Ag(I) ions. Corresponding bond paths are omitted for clarity (b). Contour line plot of the electron density ρ, bond paths connecting (3,-3) and (3,-1) critical points and starting from the Ag^I ions. Numbers show electron density at the (3,-1) critical points located on the bond path connecting Ag^I ions. Selected (3,-1) critical points are shown in blue, (3,+1) critical points are shown in orange (c). Contour line plot of the of the Laplacian of electron density ∇2ρ(r), the solid (red) and dashed (blue) lines corresponds to positive and negative values of ∇2ρ(r) respectively. Numbers show electron density at the (3,-1) critical points located on the bond path connecting Ag^I ions. Selected (3,-1) critical points are shown in blue, (3,+1) critical points are shown in orange.

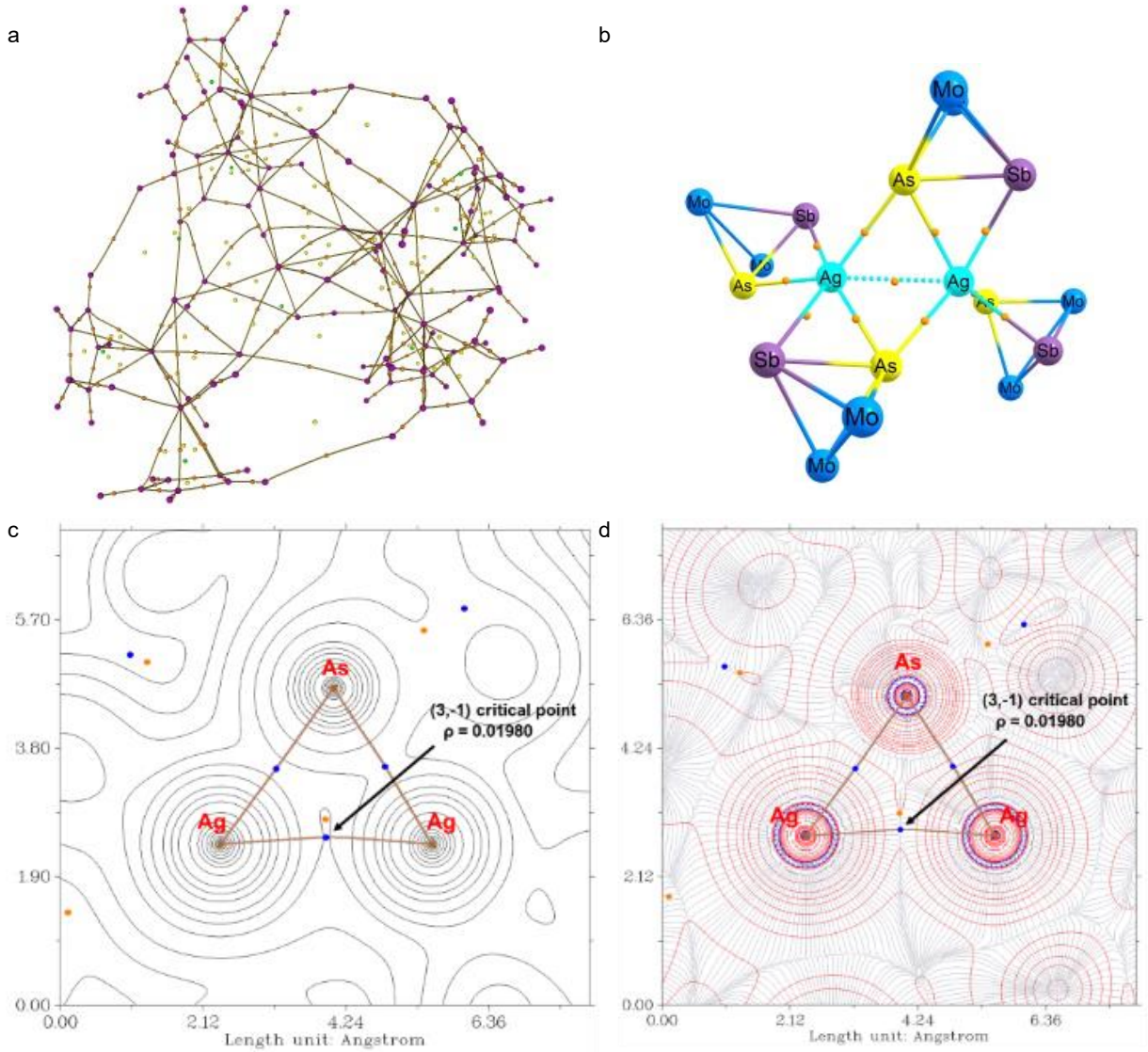

Figure S11 Summary of the QTAIM analysis of the complex $[\mu_{As},\eta^{2:1}\text{-}\mathbf{C})_2(\eta^2\text{-}\mathbf{C})_2Ag_2]^{2+}$. Molecular graph, showing the bond (3,-3) (purple), (3,-1) (orange), (3,+1) (yellow) and (3,+3) (green) critical points (a). Heavy atom core of the complex overlayed with selected (3,-1) bond critical points closest to the Ag^I ions. Corresponding bond paths are omitted for clarity (b). Contour line plot of the electron density ρ, bond paths connecting (3,-3) and (3,-1) critical points and starting from the Ag^I ions. Numbers show electron density at the (3,-1) critical points located on the bond path connecting Ag^I ions. Selected (3,-1) critical points are shown in blue, (3,+1) critical points are shown in orange (c). Contour line plot of the of the Laplacian of electron density ∇2ρ(r), the solid (red) and dashed (blue) lines corresponds to positive and negative values of ∇2ρ(r) respectively. Numbers show electron density at the (3,-1) critical points located on the bond path connecting Ag^I ions. Selected (3,-1) critical points are shown in blue, (3,+1) critical points are shown in orange.

4.6. Optimized geometries

Tables S12-S14 contain the optimized xyz coordinates of species $[(C_5H_5)_2Mo_2(CO)_4(\mu,\eta^2\text{-AsSb})]$ (**C**) (B3LYP/def2-TZVP level of theory), $[(\mu_{Sb},\eta^{2:1}\text{-}\mathbf{C})_2(\eta^2\text{-}\mathbf{C})_2Ag_2]^{2+}$.(BP86/def2-SVP level of theory, with GD3BJ), and $[(\mu_{As},\eta^{2:1}\text{-}\mathbf{C})_2(\eta^2\text{-}\mathbf{C})_2Ag_2]^{2+}$.(BP86/def2-SVP level of theory, with GD3BJ). These geometries can be also obtained from a multi-XYZ file "geometries.xyz" supplemented together with the supporting information.

Table S12 Cartesian coordinates of the gas-phase optimized geometry of $[(C_5H_5)_2Mo_2(CO)_4(\mu,\eta^2\text{-AsSb})]$ (**C**) calculated at the B3LYP/def2-TZVP level of theory. E° = -3453.70910403 Hartree.

Atom	x	y	z
Mo	1.595673000000	0.280684000000	0.134476000000
C	1.517221000000	2.643834000000	-0.382554000000
H	0.611656000000	3.223635000000	-0.395817000000
C	3.298110000000	1.369939000000	-1.068385000000
H	3.980968000000	0.814515000000	-1.690218000000
C	3.470202000000	1.650984000000	0.320005000000
H	4.310171000000	1.362010000000	0.929321000000
C	2.358948000000	2.433701000000	0.737698000000
H	2.205347000000	2.828071000000	1.729046000000
C	2.094494000000	1.980946000000	-1.498172000000
H	1.698521000000	1.969899000000	-2.499288000000
C	2.814481000000	-1.281390000000	0.071711000000
C	1.364972000000	-0.040268000000	2.075266000000
O	3.616073000000	-2.105178000000	0.025610000000
O	1.322509000000	-0.117547000000	3.227517000000
As	0.161889000000	-0.830110000000	-1.758423000000
Mo	-1.569733000000	0.383039000000	-0.021958000000
C	-1.482916000000	1.645057000000	2.043779000000
H	-0.576335000000	2.012548000000	2.491719000000
C	-3.299491000000	0.325066000000	1.567450000000
H	-4.011426000000	-0.483784000000	1.587474000000
C	-3.420886000000	1.525562000000	0.807594000000
H	-4.243024000000	1.793541000000	0.165313000000
C	-2.287650000000	2.333458000000	1.103750000000
H	-2.097082000000	3.317752000000	0.707546000000
C	-2.104898000000	0.399403000000	2.327650000000
H	-1.752389000000	-0.335028000000	3.031431000000
C	-2.788695000000	-0.725715000000	-1.126788000000
C	-1.311631000000	1.554640000000	-1.597562000000
O	-3.580678000000	-1.316811000000	-1.713315000000
O	-1.247190000000	2.316552000000	-2.461780000000
Sb	-0.172108000000	-2.001831000000	0.437897000000

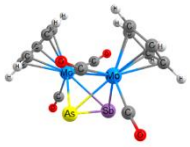

Table S13 Cartesian coordinates of the gas-phase optimized geometry of $[(\mu_{Sb},\eta^{2:1}\text{-}\mathbf{C})_2(\eta^2\text{-}\mathbf{C})_2Ag_2]^{2+}$ calculated at the BP86/def2-SVP level of theory (with GD3BJ). E°= -14106.3005711 Hartree.

Atom	x	y	z
Sb	-0.153455000000	2.467402000000	1.225390000000
Sb	3.775084000000	0.791511000000	-1.742664000000
Mo	-0.786456000000	-4.603373000000	1.327074000000
Sb	-2.527099000000	0.027603000000	-2.378108000000
Mo	-0.778845000000	-3.091959000000	4.117982000000
Mo	5.218729000000	-1.599470000000	-1.634777000000
Mo	-4.229680000000	2.355325000000	-2.327035000000
Mo	3.232159000000	-0.903591000000	-3.996188000000
Ag	-1.531494000000	-0.300567000000	0.389855000000
Sb	0.406252000000	-2.019261000000	1.814109000000
Mo	0.839062000000	3.374325000000	3.683202000000
Mo	-5.266095000000	-0.613560000000	-2.213423000000
Ag	1.531041000000	0.362922000000	0.118720000000
Mo	1.519849000000	4.803160000000	0.941888000000
As	-2.202698000000	-2.495412000000	1.913985000000
As	-3.963327000000	0.761980000000	-0.289310000000
As	2.517445000000	-1.533865000000	-1.569494000000
As	2.445375000000	2.477615000000	1.707672000000
O	-0.427265000000	-3.610423000000	-1.628914000000
O	2.302913000000	-5.157630000000	1.625383000000
O	-4.503768000000	-3.103472000000	-0.467727000000
O	3.770216000000	4.092603000000	4.581372000000
O	4.248000000000	-4.591430000000	-1.812878000000
O	-3.639042000000	1.882704000000	-5.386243000000
O	4.736118000000	-1.655366000000	1.471307000000
O	5.249022000000	1.293695000000	-5.010804000000
O	1.462041000000	0.456359000000	4.655645000000
O	-3.686642000000	-4.196773000000	4.606978000000
O	-1.388703000000	3.647036000000	-2.043721000000
C	-0.521302000000	-3.917596000000	-0.502376000000
O	-1.835333000000	-0.239887000000	4.906300000000
C	1.173891000000	-4.866974000000	1.529666000000
C	4.865155000000	-1.629194000000	0.310046000000
C	4.539669000000	-3.461331000000	-1.747265000000
C	-2.627523000000	-3.772351000000	4.358027000000
O	-7.400704000000	0.212353000000	-0.049416000000
C	4.505358000000	0.513993000000	-4.553965000000
C	-3.823854000000	1.984767000000	-4.236368000000
C	-4.740861000000	-2.127979000000	-1.068506000000
O	0.816688000000	1.092631000000	-4.214321000000
C	2.708226000000	3.813594000000	4.184003000000
C	1.466980000000	-3.497975000000	4.819372000000
H	2.370762000000	-3.249368000000	4.249419000000
C	6.965113000000	-1.257153000000	-3.249237000000
H	6.820314000000	-1.098492000000	-4.323661000000
C	1.240508000000	1.525523000000	4.235607000000
C	3.928517000000	-3.012621000000	-4.915826000000
H	4.750644000000	-3.635792000000	-4.547533000000
C	-2.363867000000	-5.958352000000	0.275647000000
H	-2.865736000000	-5.657451000000	-0.652056000000
C	7.381240000000	-2.279308000000	-1.199875000000
H	7.616593000000	-3.038218000000	-0.443395000000
C	-2.863161000000	-5.741230000000	1.600544000000
H	-3.813119000000	-5.258162000000	1.859234000000
C	-2.409538000000	3.085727000000	-2.144447000000
C	0.794849000000	-4.766652000000	4.814833000000
H	1.091199000000	-5.647507000000	4.234131000000
C	-0.281930000000	-3.390033000000	6.351489000000
H	-0.948810000000	-3.045932000000	7.152023000000
C	-6.556203000000	-0.052808000000	-0.811825000000
C	-5.507720000000	-2.286162000000	-3.821770000000
H	-4.934912000000	-3.221804000000	-3.794209000000
C	7.330742000000	-0.853795000000	-0.991824000000
H	7.511716000000	-0.336186000000	-0.041053000000
C	-1.121948000000	-6.685266000000	0.376572000000
H	-0.512164000000	-7.052097000000	-0.458458000000
C	-0.866066000000	-6.910856000000	1.773380000000
H	-0.017726000000	-7.472689000000	2.185398000000
C	4.026425000000	-1.995499000000	-5.918871000000
H	4.941226000000	-1.693814000000	-6.445360000000
C	-1.459106000000	-1.290990000000	4.559173000000
C	-1.939726000000	-6.336000000000	2.525613000000
H	-2.062521000000	-6.387823000000	3.612758000000
C	0.805601000000	-2.647450000000	5.765910000000
H	1.104759000000	-1.623483000000	6.018534000000
C	7.149285000000	-2.519214000000	-2.599765000000
H	7.167839000000	-3.501018000000	-3.090287000000
C	7.071883000000	-0.225908000000	-2.255216000000
H	7.043038000000	0.853293000000	-2.449112000000
C	1.795271000000	-2.186717000000	-5.306272000000
H	0.705819000000	-2.060095000000	-5.279074000000
C	2.707831000000	-1.480991000000	-6.172179000000
H	2.441284000000	-0.730433000000	-6.926738000000
C	-0.283356000000	-4.699355000000	5.753559000000
H	-0.961816000000	-5.520795000000	6.018324000000
C	2.550525000000	-3.125959000000	-4.531409000000
H	2.141835000000	-3.840890000000	-3.807204000000
C	-5.151519000000	-1.103469000000	-4.548420000000
H	-4.266186000000	-0.972167000000	-5.182320000000

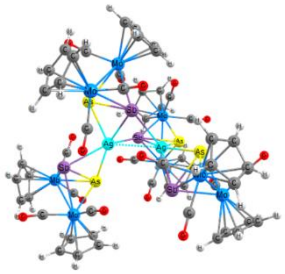

C	1.746521000000	0.398100000000	-4.076767000000
C	-6.784381000000	-2.057570000000	-3.190445000000
H	-7.361182000000	-2.785789000000	-2.606518000000
C	-6.530733000000	3.007509000000	-2.076510000000
H	-7.391969000000	2.330234000000	-2.095974000000
C	0.311703000000	5.064336000000	5.221721000000
H	1.040112000000	5.801576000000	5.583504000000
C	-4.815967000000	4.367334000000	-1.301866000000
H	-4.131715000000	4.906273000000	-0.633925000000
C	-6.207165000000	-0.144585000000	-4.379491000000
H	-6.264974000000	0.836891000000	-4.862452000000
C	-4.900245000000	4.530347000000	-2.732432000000
H	-4.304706000000	5.220561000000	-3.342933000000
C	-0.602221000000	5.246323000000	4.134794000000
H	-0.701025000000	6.144786000000	3.515672000000
C	-5.959655000000	3.680485000000	-3.204146000000
H	-6.305416000000	3.607079000000	-4.243406000000
C	-7.206590000000	-0.727819000000	-3.539258000000
H	-8.160033000000	-0.264877000000	-3.253567000000
C	-5.821038000000	3.426917000000	-0.901671000000
H	-6.051414000000	3.124675000000	0.127414000000
C	-1.419528000000	4.070178000000	4.043314000000
H	-2.255944000000	3.925215000000	3.348944000000
C	-1.015906000000	3.162059000000	5.078434000000
H	-1.471796000000	2.186627000000	5.290577000000
C	0.057804000000	3.778035000000	5.816286000000
H	0.552081000000	3.370628000000	6.707128000000
O	-1.460136000000	5.785327000000	0.648301000000
C	2.295033000000	6.796619000000	0.062231000000
H	1.898815000000	7.216818000000	-0.870663000000
C	-0.383504000000	5.336845000000	0.768324000000
C	2.668876000000	6.403415000000	2.323398000000
H	2.611945000000	6.474417000000	3.414789000000
C	3.428097000000	5.912067000000	0.186878000000
H	4.041859000000	5.532760000000	-0.639943000000
C	1.830474000000	7.092011000000	1.390543000000
H	1.006738000000	7.772003000000	1.643626000000
C	3.652006000000	5.667259000000	1.579932000000
H	4.466038000000	5.070583000000	2.009505000000
O	1.636439000000	3.842979000000	-2.044184000000
C	1.527125000000	4.135320000000	-0.920695000000

Table S14 Cartesian coordinates of the gas-phase optimized geometry of $[(\mu_{As},\eta^{2:1}\text{-}\mathbf{C})_2(\eta^2\text{-}\mathbf{C})_2Ag_2]^{2+}$ calculated at the BP86/def2-SVP level of theory (with GD3BJ). E°= -14106.3047314 Hartree.

Atom	x	y	z
Mo	0.207798000000	4.680166000000	0.193758000000
Mo	-0.075537000000	3.839967000000	3.232393000000
Mo	-5.605136000000	0.572541000000	-1.339329000000
Mo	4.268507000000	-2.117852000000	-2.461865000000
Mo	-3.958553000000	-0.660968000000	-3.752427000000
Mo	0.023174000000	-2.707560000000	4.077938000000
Mo	5.301919000000	0.838567000000	-2.244165000000
Ag	-1.493886000000	-0.414714000000	0.258019000000
Mo	-0.430163000000	-4.559326000000	1.488415000000
O	0.552134000000	2.968690000000	-2.413821000000
O	-2.915276000000	4.422301000000	-0.087533000000
O	5.061593000000	3.062566000000	-0.047492000000
O	-2.367690000000	-4.049861000000	5.643837000000
O	-5.491482000000	3.383303000000	-2.760483000000
O	3.069025000000	-1.332409000000	-5.265490000000
O	-4.662090000000	1.838512000000	1.375081000000
O	-5.564373000000	-3.342786000000	-3.377012000000
O	-1.333885000000	0.007668000000	4.871989000000
O	2.264747000000	5.857800000000	3.841403000000
O	1.474230000000	-3.374262000000	-1.810089000000
C	0.415421000000	3.548431000000	-1.405505000000
O	1.467256000000	1.712229000000	4.950159000000
C	-1.754731000000	4.450239000000	0.062021000000
C	-4.952037000000	1.382346000000	0.336219000000
C	-5.448672000000	2.335479000000	-2.243105000000
C	1.439088000000	5.083217000000	3.549562000000
O	7.849986000000	-0.306225000000	-0.787232000000
C	-4.963950000000	-2.342134000000	-3.445929000000
C	3.497263000000	-1.557992000000	-4.201540000000
C	5.117857000000	2.176650000000	-0.812484000000
O	-1.304603000000	-2.342463000000	-3.754480000000
C	-1.526160000000	-3.568002000000	5.001159000000
C	-2.451740000000	3.688927000000	3.472560000000
H	-3.110236000000	3.065337000000	2.854580000000
C	-7.481473000000	-0.614012000000	-2.261522000000
H	-7.500754000000	-1.116506000000	-3.235154000000
C	-0.860845000000	-0.997920000000	4.508201000000
C	-5.220468000000	0.828468000000	-5.155536000000
H	-6.063897000000	1.451712000000	-4.838833000000
C	1.593343000000	6.144305000000	-0.978811000000
H	2.308662000000	5.801945000000	-1.736871000000
C	-7.755174000000	0.983002000000	-0.592276000000
H	-8.028196000000	1.909917000000	-0.072662000000
C	1.884726000000	6.374083000000	0.405951000000
H	2.861162000000	6.252943000000	0.890701000000
C	2.495663000000	-2.844505000000	-2.021798000000
C	-2.145765000000	5.071481000000	3.243624000000
H	-2.534714000000	5.686207000000	2.424178000000
C	-1.099016000000	4.427581000000	5.217538000000
H	-0.548468000000	4.468241000000	6.165885000000
C	6.855878000000	0.069145000000	-1.275174000000
C	5.166937000000	2.698418000000	-3.644156000000
H	4.605701000000	3.600428000000	-3.371442000000
C	-7.311803000000	-0.243048000000	0.024258000000
H	-7.179317000000	-0.410618000000	1.100747000000
C	0.219612000000	6.510831000000	-1.216805000000
H	-0.295803000000	6.508730000000	-2.185318000000
C	-0.328449000000	6.962590000000	0.033995000000
H	-1.343005000000	7.354264000000	0.183068000000
C	-5.302428000000	-0.504792000000	-5.669433000000
H	-6.222035000000	-1.087603000000	-5.809388000000
C	0.926513000000	2.483533000000	4.254440000000
C	0.696862000000	6.885720000000	1.029068000000
H	0.613324000000	7.218952000000	2.068819000000
C	-1.809056000000	3.289416000000	4.690640000000
H	-1.877114000000	2.298229000000	5.153758000000
C	-7.852921000000	0.744854000000	-2.006792000000
H	-8.205141000000	1.468525000000	-2.753231000000
C	-7.140559000000	-1.223328000000	-1.007064000000
H	-6.861332000000	-2.274014000000	-0.861659000000
C	-3.077632000000	0.157774000000	-5.748931000000
H	-1.999953000000	0.174440000000	-5.955925000000
C	-3.979019000000	-0.927776000000	-6.045095000000
H	-3.716397000000	-1.877602000000	-6.527478000000
C	-1.305951000000	5.525288000000	4.311207000000
H	-0.933877000000	6.548482000000	4.450866000000
C	-3.844850000000	1.237548000000	-5.199536000000
H	-3.464282000000	2.229887000000	-4.928697000000
C	4.667376000000	1.599058000000	-4.415747000000
H	3.658539000000	1.509439000000	-4.836506000000
C	-2.291133000000	-1.718269000000	-3.699176000000
C	6.555059000000	2.443020000000	-3.345755000000
H	7.241290000000	3.114166000000	-2.814095000000
C	6.566364000000	-2.765743000000	-2.772408000000
H	7.411104000000	-2.082611000000	-2.913093000000
C	1.258383000000	-3.829331000000	5.721626000000
H	0.860890000000	-4.689884000000	6.275235000000
C	5.041105000000	-4.208682000000	-1.779730000000
H	4.513381000000	-4.808630000000	-1.027485000000
C	5.741202000000	0.666087000000	-4.605278000000
H	5.694188000000	-0.255138000000	-5.196163000000
C	4.816372000000	-4.235632000000	-3.203798000000
H	4.100363000000	-4.872434000000	-3.738207000000
C	2.060911000000	-3.897412000000	4.538175000000
H	2.377138000000	-4.817456000000	4.033187000000
C	5.760839000000	-3.334900000000	-3.808735000000
H	5.878598000000	-3.161757000000	-4.886323000000
C	6.898967000000	1.180188000000	-3.938806000000
H	7.894914000000	0.718739000000	-3.926863000000
C	6.118533000000	-3.299064000000	-1.516958000000
H	6.576191000000	-3.104185000000	-0.539556000000
C	2.406943000000	-2.561938000000	4.151575000000
H	3.044587000000	-2.284071000000	3.303657000000
C	1.828252000000	-1.658959000000	5.103894000000
H	1.938724000000	-0.567155000000	5.113890000000
C	1.118315000000	-2.444186000000	6.085793000000
H	0.614140000000	-2.059068000000	6.981281000000
Sb	2.074576000000	3.030704000000	1.490175000000
As	-0.426977000000	2.237631000000	1.198966000000

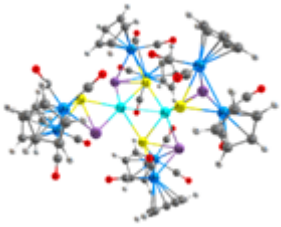

As	2.792071000000	0.117943000000	-2.040785000000
Sb	4.278620000000	-0.711340000000	-0.038245000000
C	-2.010691000000	-6.211007000000	0.941341000000
H	-2.641257000000	-6.711871000000	1.687109000000
C	-0.259529000000	-5.734381000000	-0.513598000000
H	0.678924000000	-5.799855000000	-1.076215000000
C	-2.373688000000	-5.064284000000	0.162474000000
H	-3.343381000000	-4.551710000000	0.185042000000
C	-1.287046000000	-4.761905000000	-0.726831000000
H	-1.248304000000	-3.946213000000	-1.459248000000
O	-0.296571000000	-6.324881000000	4.071310000000
C	-0.698149000000	-6.634521000000	0.520668000000
H	-0.160831000000	-7.521069000000	0.880462000000
C	-0.334975000000	-5.546146000000	3.195164000000
C	1.541945000000	-4.583013000000	1.398473000000
O	2.702877000000	-4.668926000000	1.262996000000
As	0.333579000000	-2.003421000000	1.522078000000
Sb	-2.163985000000	-2.471684000000	2.275185000000
Ag	1.543801000000	0.342774000000	0.439040000000
As	-3.796160000000	-1.289198000000	-1.135992000000
Sb	-2.805776000000	1.050970000000	-1.861933000000

5. References:

[1] L. Dütsch, C. Riesinger, G. Balazs and M. Scheer, *Chem. Eur. J.,* 2021, **27**, 8804-8810.

[2] M. Elsayed Moussa, M. Piesch, M. Fleischmann, A. Schreiner, M. Seidl and M. Scheer, *Dalton Trans.,* 2018, **47**, 16031-16035.

[3] T. Köchner, N. Trapp, T. A. Engesser, A. J. Lehner, C. Röhr, S. Riedel, C. Knapp, H. Scherer, I. Krossing, *Angew. Chem. Int. Ed*. 2011, **50**, 11253-11256; *Angew. Chem*. 2011, **123**, 11449-11452.

[4] CrysAlisPro Software System, Rigaku Oxford Diffraction, (2015-2020).

[5] R. C. Clark, J. S. Reid, **1995**. *Acta Cryst*. A51, 887-897.

[6] O. V. Dolomanov, L. J. Bourhis, R. J. Gildea. J. A. K. Howard, H. Puschmann, *J. Appl. Cryst.*, **2009**, 42, 339-341.

[7] G. M. Sheldrick, *Acta Cryst*., **2015**, A71, 3-8.

[8] G. M. Sheldrick, *Acta Cryst*., **2015**, C71, 3-8.

[9] Gaussian 09, Revision E.01, M. J. Frisch, G. W. Trucks, H. B. Schlegel, G. E. Scuseria, M. A. Robb, J. R. Cheeseman, G. Scalmani, V. Barone, B. Mennucci, G. A. Petersson, H. Nakatsuji, M. Caricato, X. Li, H. P. Hratchian, A. F. Izmaylov, J. Bloino, G. Zheng, J. L. Sonnenberg, M. Hada, M. Ehara, K. Toyota, R. Fukuda, J. Hasegawa, M. Ishida, T. Nakajima, Y. Honda, O. Kitao, H. Nakai, T. Vreven, J. A. Montgomery, Jr., J. E. Peralta, F. Ogliaro, M. Bearpark, J. J. Heyd, E. Brothers, K. N. Kudin, V. N. Staroverov, T. Keith, R. Kobayashi, J. Normand, K. Raghavachari, A. Rendell, J. C. Burant, S. S. Iyengar, J. Tomasi, M. Cossi, N. Rega, J. M. Millam, M. Klene, J. E. Knox, J. B. Cross, V. Bakken, C. Adamo, J. Jaramillo, R. Gomperts, R. E. Stratmann, O. Yazyev, A. J. Austin, R. Cammi, C. Pomelli, J. W. Ochterski, R. L. Martin, K. Morokuma, V. G. Zakrzewski, G. A. Voth, P. Salvador, J. J. Dannenberg, S. Dapprich, A. D. Daniels, O. Farkas, J. B. Foresman, J. V. Ortiz, J. Cioslowski, and D. J. Fox, Gaussian, Inc., Wallingford CT, 2013

[10] A. D. Becke, *Phys. Rev. A*, 1988, **38**, 3098-3100.

[11] a) F. Weigend and R. Ahlrichs, *Phys. Chem. Chem. Phys.*, 2005, **7**, 3297-3305; b) F. Weigend, *Phys. Chem. Chem. Phys.*, 2006, **8**, 1057-1065.

[12] S. Grimme, S. Ehrlich and L. Goerigk, *J. Comput. Chem.*, 2011, **32**, 1456-1465.

[13] T. A. Manz, *Rsc Adv*, 2017, **7**, 45552-45581.

[14] R. F. W. Bader and H. Essen, *J. Chem. Phys.*, 1984, **80**, 1943-1960.

[15] T. Lu and Q. X. Chen, *Chem. Methods*, 2021, **1**, 231-239.

[16] T. Lu and F. W. Chen, *J. Comput. Chem.*, 2012, **33**, 580-592.

[17] a) P. J. Stephens, F. J. Devlin, C. F. Chabalowski and M. J. Frisch, *J. Phys. Chem.*, 1994, **98**, 11623-11627; b) A. D. Becke, *J. Chem. Phys.*, 1993, **98**, 5648-5652; c) C. T. Lee, W. T. Yang and R. G. Parr, *Phys. Rev. B*, 1988, **37**, 785-789; d) S. H. Vosko, L. Wilk and M. Nusair, *Can. J. Phys.*, 1980, **58**, 1200-1211.

[18] NBO 7.0. E. D. Glendening, J, K. Badenhoop, A. E. Reed, J. E. Carpenter, J. A. Bohmann, C. M. Morales, P. Karafiloglou, C. R. Landis, and F. Weinhold, Theoretical Chemistry Institute, University of Wisconsin, Madison, 2018. (https://nbo6.chem.wisc.edu/biblio_css.htm)

[19] a) M. Elsayed Moussa, J. Schiller, E. Peresypkina, M. Seidl, G. Balazs, P. A. Shelyganov and M. Scheer, *Chem. Eur. J.*, 2020, **26**, 14315-14319; b) P. A. Shelyganov, M. Elsayed Moussa, M. Seidl and M. Scheer, *Angew. Chem. Int. Ed.*, 2023, **62**, e202215650.

[20] G. A. Zhurko and D. A. Zhurko, "ChemCraft, Tool for Treatment of the Chemical Data". http://www.chemcraftprog.com

[21] S. Shahbazian, *Chem. Eur. J.*, 2018, **24**, 5401-5405.